

## Antiprotonic atoms in gaseous $\text{H}_2$ and He and in liquid $\text{H}_2$

J. R. Lindemuth,\* M. Eckhause, K. L. Giovanetti,<sup>†</sup> J. R. Kane, M. S. Pandey,<sup>‡</sup> A. M. Rushton,<sup>§</sup>  
W. F. Vulcan, R. E. Welsh, and R. G. Winter  
*College of William and Mary, Williamsburg, Virginia 23185*

P. D. Barnes, J. N. Craig,\*\* R. A. Eisenstein, J. D. Sherman,<sup>††</sup> R. B. Sutton, and W. R. Wharton  
*Carnegie Mellon University, Pittsburgh, Pennsylvania 15213*

J. P. Miller and B. L. Roberts  
*Boston University, Boston, Massachusetts 02215*

A. R. Kunselman  
*University of Wyoming, Laramie, Wyoming 82071*

R. J. Powers  
*California Institute of Technology, Pasadena, California 91125*  
(Received 14 March 1984)

Antiprotons were brought to rest in targets of gaseous  $\text{H}_2$  and gaseous He at temperatures of 30 K and also in a target of liquid  $\text{H}_2$ . High-resolution x-ray detectors were used to measure the energies of x rays from  $\bar{p}$ -He and to search for x rays from  $\bar{p}$ -H. The  $\bar{p}$ -He data are compared with similar measurements at different densities and with the theoretical predictions of Landua and Klempt. The  $\bar{p}$ -H data provide upper limits for the yields of  $nP \rightarrow 1S$  x rays in liquid and gaseous hydrogen.

Antiprotonic atoms were first observed at the Centre Européen de Recherche Nucléaires (CERN)<sup>1</sup> in 1970 and, since that time, in various experiments at Argonne, Brookhaven, and CERN. Recent reviews of the experimental data and of their interpretation have been given by Batty<sup>2</sup> and by Poth.<sup>3</sup> Although it is expected that better data will be available soon from the low-energy antiproton ring (LEAR) at CERN, we present here a brief summary of some older results for  $\bar{p}$ -He and  $\bar{p}$ -H atoms to facilitate comparison.

We used the low-energy separated beam LESB I at the Brookhaven alternating gradient synchrotron (AGS) to bring antiprotons to rest in targets of liquid  $\text{H}_2$  ( $\text{LH}_2$ ) and gaseous  $\text{H}_2$  and He at temperatures of 30 K. The target volume was viewed by two high-resolution Si(Li) detectors. Detectors of 300  $\text{mm}^2$  area and 300 eV resolution (full width at half maximum) at 5.9 keV were used for part of the experiment while larger detectors (750  $\text{mm}^2$ ) of poorer resolution (450 eV) were used for another part. Antiprotons were identified by time of flight information while negative pions and muons in the beam were rejected by means of a threshold Cherenkov detector. About 1% of the beam was antiprotons. Approximately 5000  $\bar{p}$ /s of momentum 620 MeV/c were incident on the counter array. Of these, 1500/s emerged from the degrader. About 150  $\bar{p}$ /s were stopped in the gaseous targets and about 1000  $\bar{p}$ /s were stopped in the liquid  $\text{H}_2$  target. The target vessel was a cylinder approximately 17 cm in diameter by 17 cm high with 0.35 mm Mylar walls. The Si(Li) detectors viewed the target volume through Mylar windows 75  $\mu\text{m}$  thick. For the latter part of the experiment, the target vessel was lined with Ag foil 125  $\mu\text{m}$  thick to attenuate  $\bar{p}$  x rays from the Mylar walls. Contaminant  $\bar{p}$  x rays from Ag in the energy range of interest were of very low yield owing to the Auger effect. The

detector windows were also replaced in the latter part of the experiment with 25  $\mu\text{m}$  Mylar supported on a grid of 75  $\mu\text{m}$  Mylar so as to enhance transmission of low-energy photons. Pulses from the Si(Li) detectors were digitized in a 1024 channel ADC and the resulting histograms were stored in a PDP 11-34 computer or in a separate memory interfaced to a magnetic tape unit. Calibration sources of  $^{57}\text{Co}$  and  $^{78}\text{Ge}$  were mounted so that they could be positioned in view of the detectors for beam-on calibration or shielded for the accumulation of  $\bar{p}$  x-ray spectra free of calibration lines. The detectors' relative efficiencies and window transmission functions were obtained under running conditions from calculated relative yields of the  $\bar{p}$ -C x-ray lines.<sup>4</sup> The Si(Li) spectrometer systems exhibited good stability throughout the run. Figure 1 shows the data obtained from antiprotons stopped in gaseous He at 30 K. The  $\bar{p}$ - $\text{H}_2$  gas target data are shown in Fig. 2, and the  $\bar{p}$ - $\text{LH}_2$  data are shown in Fig. 3. The relatively low contamination from background lines in the  $\bar{p}$   $\text{LH}_2$  data is due to the reduced fraction of  $\bar{p}$  stops in Mylar when the more dense  $\text{LH}_2$  target was used.

A major goal of the experiment was the measurement of strong-interaction effects in the proton-antiproton atomic system. The  $\bar{p}$ - $\text{H}_2$  data were therefore analyzed for evidence of  $nP \rightarrow 1S$  x rays. Because such x rays have not as yet been unambiguously observed, and because their strong-interaction shifts and widths have not been predicted consistently by theory, one is obliged to search for the presence of such x rays over an energy range of several keV both below and above the calculated Dirac energy of 9.3 keV for the  $2P-1S$  transition. In addition, the separate spin-isospin states of the  $1S\bar{p}$ -p system can be both shifted and broadened differently from each other.<sup>5</sup> Accordingly, a search was made for x-ray lines throughout the energy region 5–15 keV. In this search, both the widths and the in-

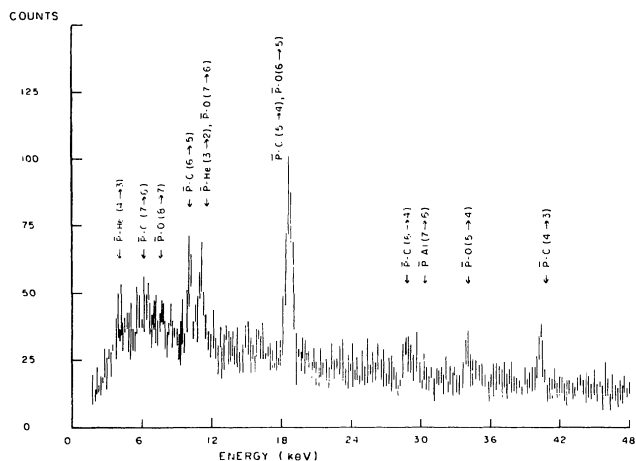


FIG. 1. The  $\bar{p}$  x-ray spectrum from gaseous helium at 30 K. The  $\bar{p}$  carbon and  $\bar{p}$  oxygen peaks are caused by stops in the Mylar lining of the target.

tensities of the x-ray lines were free parameters.

For most of the analysis of the gaseous  $\bar{p}$ -H<sub>2</sub> data, the background was taken to be the  $\bar{p}$ -He spectrum with the He lines ignored. For this subtraction, the 5 $\rightarrow$ 4 $\bar{p}$ -C line at 18.6 keV was used for normalization. The resulting spectrum, shown in Fig. 4, was then subjected to an analysis which consisted of moving a Gaussian of various fixed widths (ranging from the minimum of the instrumental width up to 1 keV) across the spectrum and mapping the resulting chi-squared distribution. In addition, the technique described by Izycki *et al.*<sup>6</sup> was tried. In this approach, the data were tested for the presence of three peaks (2 $p \rightarrow$  1s, 3 $p \rightarrow$  1s, 4 $p \rightarrow$  1s) whose absolute energies were considered unknown but whose relative energy separations were held fixed at the 3 $\rightarrow$  2 (1.74 keV) and 4 $\rightarrow$  2 (2.34 keV)  $\bar{p}$ -p electromagnetic energies. The peak widths were held fixed for each sweep while the relative peak amplitudes were free. In addition, a similar two-Gaussian sweep was made with the separation held fixed at the 3 $\rightarrow$  2 electromagnetic energy difference. The raw  $\bar{p}$ -H<sub>2</sub> gas data were also subjected to

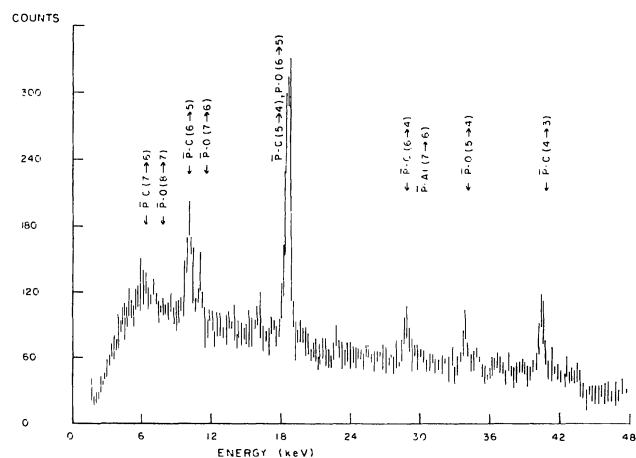


FIG. 2. The  $\bar{p}$  x-ray spectrum from gaseous hydrogen at 30 K.

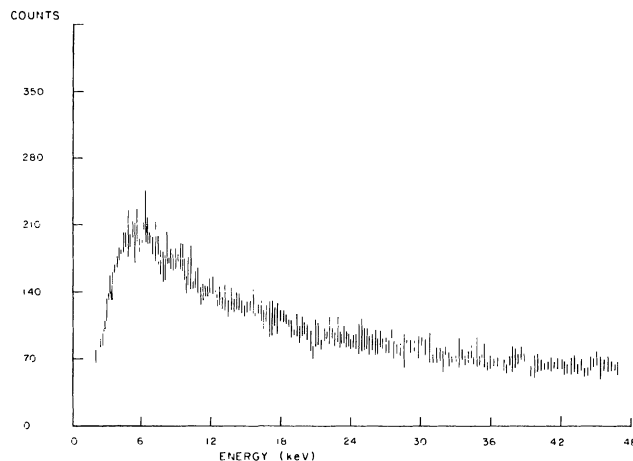


FIG. 3. The  $\bar{p}$  x-ray spectrum from liquid hydrogen. No identifiable x-ray peaks were found.

such an analysis without the  $\bar{p}$ -He background subtraction but the presence of the  $\bar{p}$ -C and  $\bar{p}$ -O lines made such a fit less useful. The  $\bar{p}$ -LH<sub>2</sub> data were fitted without background subtraction.

The  $\bar{p}$ -He data were fitted freely except for the 3 $\rightarrow$  2 transition which was contaminated by the presence of the  $\bar{p}$ -O 7 $\rightarrow$  6 line. This contaminant was extracted both by comparison with the  $\bar{p}$ -O 7 $\rightarrow$  6 line in the H<sub>2</sub> gas data and by direct subtraction of the entire  $\bar{p}$ -H<sub>2</sub> spectrum based on normalization at the  $\bar{p}$ -C 5 $\rightarrow$  4 x ray. These two methods of normalization yielded consistent results within the statistical errors. Evident in the  $\bar{p}$ -He gas data taken at 30 K (Fig. 1) is the  $\bar{p}$ -He 3 $\rightarrow$  2 transition at 11.1 keV along with contaminant lines from  $\bar{p}$ -C and  $\bar{p}$ -O arising from  $\bar{p}$  stops in Mylar. The  $\bar{p}$ -He 4 $\rightarrow$  3, 5 $\rightarrow$  3, and 6 $\rightarrow$  3 are also present although the counting rate for the 4 $\rightarrow$  3 transition is reduced because of low detector efficiency and low x-ray transmission through the target and windows at that energy.

The yields of the  $\bar{p}$ -He transitions measured in this work

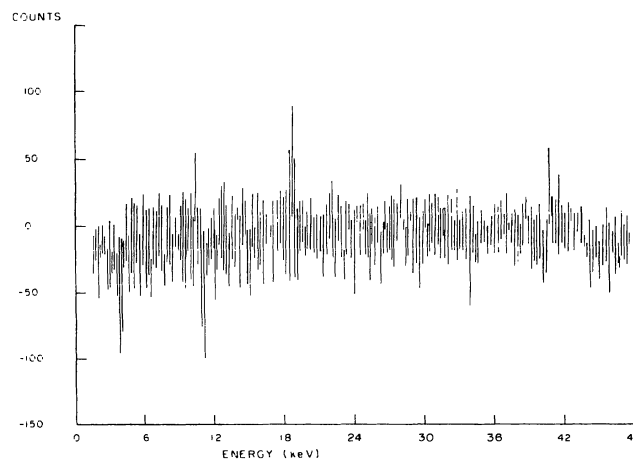


FIG. 4. The background-subtracted  $\bar{p}$  x-ray spectrum from gaseous hydrogen. The normalized difference between Figs. 2 and 1 was based on the  $\bar{p}$ C(5 $\rightarrow$  4) line. No peaks that can be attributed to hydrogen can be discerned in the result.

TABLE I. X-ray yields in  $\bar{p}$ -He (gas,  $T=30$  K).

Transition	$E$ (keV)	Absolute yield	Yield relative to $3 \rightarrow 2$
$4 \rightarrow 3$	$3.97 \pm 0.04$	$0.06 \pm 0.03$	$1.50 \pm 0.30$
$5 \rightarrow 3$	$5.78 \pm 0.07$	$0.03 \pm 0.02$	$0.75 \pm 0.37$
$6 \rightarrow 3$	$6.53 \pm 0.06$	$0.03 \pm 0.02$	$0.75 \pm 0.31$
$3 \rightarrow 2$	$11.14 \pm 0.03$	$0.04 \pm 0.02$	1
$4 \rightarrow 2$	$15.02 \pm 0.14$	$0.01 \pm 0.01$	$0.25 \pm 0.63$

are shown in Table I. These yields provide information on the strong-interaction capture rate of antiprotons from the 3D atomic state in He. Because of uncertainties in the mean solid angles seen by the detectors, the errors on the absolute yields are substantially greater than the errors on the relative yields. Note that the 3D capture width is determined from yields relative to that of the  $3 \rightarrow 2$  transition, and that it does not depend on the absolute yields. The absolute yield of the  $\bar{p}$ -He  $3 \rightarrow 2$  transition is of particular interest. This yield should depend on the density of the He. After initial atomic capture of the  $\bar{p}$  by a He atom, the two  $e^-$  are ejected and the  $(\bar{p}\text{He})^+$  system deexcites primarily via the external Auger effect, with a rate that depends linearly on the density of He. For transitions between  $\bar{p}$ -He atomic states of relatively low ( $4-7$ )  $n$ , the radiative process begins to dominate, particularly for low densities. Since radiation tends to "circularize" the deexcitation, one would expect that the ratio  $L_\alpha/L_{\text{total}}$  for  $\bar{p}$  atoms formed in gaseous He would be larger than that for  $\bar{p}$  atoms formed liquid He. In Table II are listed the absolute  $\bar{p}$ -He  $3 \rightarrow 2$  x-ray yields measured for different He densities, as well as the strong-interaction capture widths obtained for the 3D state, which has a radiation width of  $1.44 \times 10^{-3}$  eV. In these experiments the relative yields of transitions to and from the 3D state were determined with only limited accuracy owing to both limited statistics and to the uncertainty in the large attenuation of the  $4 \rightarrow 3\bar{p}$ -He x ray at 3.97 keV. From our  $\bar{p}$ -He data, summarized in Table I, we obtain a capture width from the 3D state of  $(3 \pm 1) \times 10^{-3}$  eV.

Landua and Klempt<sup>7</sup> have carried out cascade calculations that have explained satisfactorily the relatively high  $K_\beta/K_\alpha$  intensity ratio measured for pionic atoms formed in liquid He. These calculations have also been made for  $\bar{p}$ -He and are discussed by Wodrich *et al.*,<sup>8</sup> who compared their experimental results at 1.1 and 4 atm pressure to the liquid He experimental results (equivalent to 700 atm) of Poth *et al.*<sup>9</sup> The results presented here for He gas at 30 K and 1 atm

TABLE II. Experimental strong interaction widths in the 3D state of atomic  $\bar{p}$ -He.

	(K)	Absolute $3 \rightarrow 2$ x-ray yield	3D capture width ( $10^{-3}$ eV)	Reference
Liquid He	4	$0.044 \pm 0.022$		10
Liquid He	4	$\sim 0.01$	$0.40 \pm 0.14^a$	9
1.0 atm gas	30	$0.04 \pm 0.02$	$3 \pm 1$	This work
4.0 atm gas	300	$0.07 \pm 0.04$	$2.8 \pm 1.1^b$	8
1.1 atm gas	300	$0.08 \pm 0.08$	$> 1.5^b$	8

<sup>a</sup>Not given in Ref. 9, but obtained from the yields given therein.

<sup>b</sup>For a 3D radiative width of 1.0 meV, as used in Ref. 8. If the actual radiative width of 1.44 meV is used, the capture widths and their errors would increase proportionally.

(equivalent to 11 atm at 300 K) give a yield per  $\bar{p}$  stop for the  $\bar{p}$ -He  $3 \rightarrow 2$  transition of  $0.04 \pm 0.02$ , in good agreement with the predictions of Wodrich *et al.*<sup>8</sup> and Landua and Klempt.<sup>7</sup>

The recent work of Baird *et al.*<sup>10</sup> for liquid He gives absolute yields of  $0.044 \pm 0.022$  for the  $\bar{p}$ -He  $3 \rightarrow 2$  transition and  $0.009 \pm 0.005$  for the  $\bar{p}$ -He  $4 \rightarrow 2$  transition. The corresponding  $L_\alpha/L_\beta$  intensity ratio is in general agreement with the experimental results of Poth *et al.*<sup>9</sup> and the theoretical predictions made by Wodrich *et al.*<sup>8</sup> The absolute yields quoted by Baird *et al.*,<sup>10</sup> however, are greater than those measured by Poth *et al.*<sup>9</sup> and exceed the predictions of Wodrich *et al.*<sup>8</sup>

Analysis of the  $\bar{p}$ -H<sub>2</sub> data obtained in this experiment gives upper limits for the yield of the  $\bar{p}$ -p  $2P \rightarrow 1S$  x ray for capture widths  $\leq 1$  keV. These limits are  $1 \times 10^{-3}$  per  $\bar{p}$  stopped in gas at 30 K and  $3 \times 10^{-4}$  in LH<sub>2</sub>. Poor electronic and x-ray transmission efficiency in the 2 keV region precluded the possibility of observing in this experiment the  $L$  series  $\bar{p}$ -p x rays reported by Auld *et al.*<sup>11</sup>

We conclude that the  $\bar{p}$ -He data reported here show good agreement with the cascade predictions of Landua and Klempt.<sup>7</sup> However, the  $\bar{p}$ -H<sub>2</sub> data do not appear to confirm the presence of the weak lines reported by Izycki *et al.*<sup>6</sup>

This work is based on a dissertation<sup>4</sup> submitted by one of us (J.R.L.) to the College of William and Mary in partial fulfillment of the requirements of the Ph.D. degree and was supported by the National Science Foundation and the Department of Energy. We are indebted to R. Meier and the hydrogen target group and to the AGS division at Brookhaven National Laboratory for their hospitality and assistance.

\*Present address: EG&G Princeton Applied Research, Princeton, NJ 08540.

†Present address: Eidgenössische Technische Hochschule, c/o Schweizerisches Institut für Nuklearforschung, CH-5234 Villigen, Switzerland.

‡Present address: AT&T Technologies, Crawford Corner Rd., Holmdel, NJ 07033.

§Present address: Physics Department, University of California, Irvine, CA 90024.

\*\*Present address: CGR Medical Corporation, 2519 Wilkens Avenue, Baltimore, MD 21203.

††Present address: Los Alamos National Laboratory, Los Alamos, NM 87545.

<sup>1</sup>A. Bamberger *et al.*, Phys. Lett. **33B**, 233 (1970).

<sup>2</sup>C. J. Batty, Nucl. Phys. **A372**, 433 (1981).

<sup>3</sup>H. Poth, *Proceedings of Workshop on Physics at LEAR*, edited by U. Gastaldi (Plenum, New York, in press).

<sup>4</sup>J. L. Lindemuth, Dissertation, College of William and Mary, 1982 (unpublished).

<sup>5</sup>I. S. Shapiro, Phys. Rev. **35**, 129 (1978).

<sup>6</sup>M. Izycki *et al.*, Z. Phys. A **297**, 1 (1980).

<sup>7</sup>R. Landua and E. Klempt, Phys. Rev. Lett. **48**, 1722 (1982).

<sup>8</sup>R. W. Wodrich *et al.*, Nucl. Phys. **A384**, 386 (1982).

<sup>9</sup>H. Poth *et al.*, Phys. Lett. **76B**, 523 (1978).

<sup>10</sup>S. Baird *et al.*, Nucl. Phys. **A392**, 297 (1983).

<sup>11</sup>E. G. Auld *et al.*, Phys. Lett. **77B**, 154 (1978).